$N_{\mathrm{Te}-g}{}^0$ are assumed to be known fractions of $N_{\mathrm{Te}-m}{}^0$, and f is known, all terms on the right of Eq. (A1) except the first can be collected so that

$$A_{133}=\epsilon_{133}\lambda_{133}[\,j'N_b{}^0+N_c{}^0\exp(-\lambda_I\tau)\,]\times\exp(-\lambda_I\tau''+\lambda_I\tau),\quad\text{(A4)}$$

where j' is the sum of coefficients of $N_b{}^0$ from Eq. (A1). Rearranging,

$$A_{133}\exp(\lambda_I\tau'')=\epsilon_{133}\lambda_{133}(\,jN_b{}^0+N_c{}^0),\quad\text{(A5)}$$

where $j=j'\exp(\lambda_I\tau)$.

ACKNOWLEDGMENTS

The authors wish to thank R. M. Harbour for help with several of the irradations, R. L. Ferguson for his careful reading and editing of the first drafts of this manuscript, and L. Berge for assistance with the calculations. Most of this work was done while D.E.T. was a Visiting Scientist at Oak Ridge National Laboratory and N.G.R. was an Oak Ridge Associated Universities Summer Research Participant at the same laboratory. We are grateful for the generous support of both these organizations.

PHYSICAL REVIEW C VOLUME 1, NUMBER 1 JANUARY 1970

Neutron and Photon Emission from Ba Compound Nuclei*

V. SUBRAHMANYAM† AND MORTON KAPLAN‡

Department of Chemistry, Yale University, New Haven, Connecticut 06520

(Received 11 September 1969)

We report recoil angular distribution measurements from (C^{12}, xn) compound-nucleus reactions with Sn^{118}, Sn^{119}, Sn^{120}, and Sn^{122}. In each case, the final product investigated was Ba^{126}, corresponding to reactions in which 4, 5, 6, and 8 neutrons are emitted. The data have been analyzed to yield information on the average total energies of neutrons and photons emitted in the deexcitation of the compound nuclei. Evidence is presented for significant competition between neutron evaporation and γ-ray deexcitation processes, particularly for the $4n$ and $5n$ reactions. At the higher bombarding energies, the total energy dissipated as γ radiation is an appreciable fraction of the available decay energy.

INTRODUCTION

In the decay of highly excited compound nuclei, γ-ray emission may compete significantly with nucleon evaporation even at energies considerably above particle-emission thresholds.[1,2] This phenomenon is enhanced when compound nuclei are formed with high angular momenta, and hence is more likely to occur in nuclear reactions induced by heavy ions. A particularly convenient method for studying the γ-ray competition with particle emission is based upon angular distribution measurements of the recoiling residual nuclei.[3,4] This technique has been successfully employed to derive the energetics of nucleon and photon emission from specific compound-nucleus reactions in several areas of the Periodic Table.[3–7] Its main virtue lies in the unique identification, by the radioactive decay of product nuclei, of the reaction being studied with no interference from extraneous nuclear processes occurring in the target.

The nuclear reactions involving moderately high-Z compound nuclei are primarily of the neutron-emitting type. Such (HI, xn) reactions are useful for investigation, not only because of their large cross sections,[8,9] but also because their relative simplicity is amenable to detailed analysis. Experimental measurements of γ-ray competition in (HI, xn) reactions provide a body of data with which the recent, detailed calculations of Grover[10] and Grover and Gilat[11,12] can be compared.

* Work supported by the U.S. Atomic Energy Commission.

† Present address: Department of Chemistry, Boston College, Chestnut Hill, Mass.

‡ Alfred P. Sloan Foundation Fellow.

[1] J. R. Grover, Phys. Rev. **123**, 267 (1961).

[2] J. R. Grover, Phys. Rev. **127**, 2142 (1962).

[3] G. N. Simonoff and J. M. Alexander, Phys. Rev. **133**, B104 (1964).

[4] M. Kaplan and V. Subrahmanyam, Phys. Rev. **153**, 1186 (1967).

[5] M. Kaplan and A. Ewart, Phys. Rev. **148**, 1123 (1966).

[6] N. T. Porile and G. B. Saha, Phys. Rev. **158**, 1027 (1967).

[7] J. M. Alexander, in *Nuclear Chemistry*, edited by L. Yaffe (Academic Press Inc., New York, 1968), Chap. 4, pp. 273–357.

[8] J. M. Alexander and G. N. Simonoff, Phys. Rev. **133**, B93 (1964).

[9] M. Kaplan, Phys. Rev. **143**, 894 (1966).

[10] J. R. Grover, Phys. Rev. **157**, 832 (1967).

[11] J. R. Grover and J. Gilat, Phys. Rev. **157**, 802 (1967).

[12] J. R. Grover and J. Gilat, Phys. Rev. **157**, 823 (1967).

In the present paper, we report the results of further recoil angular distribution studies, obtained from (C^{12}, xn) reactions with Sn^{118}, Sn^{119}, Sn^{120}, and Sn^{122}. In each case, the final product investigated was Ba^{126}, corresponding to reactions in which 4, 5, 6, and 8 neutrons are emitted. These reactions, or ones very closely related to them, have been examined earlier in some detail, and strong evidence was presented to support a compound-nucleus reaction mechanism.[13]

EXPERIMENTAL PROCEDURES

The angular distribution experiments were performed using beams of C^{12} ions from the Yale heavy-ion linear accelerator. The experimental apparatus has been described elsewhere,[4] and consists of a collimation system, target holder, recoil catcher, and Faraday cup, all mounted concentric with the beam axis in a vacuum chamber. The heavy-ion beam was collimated to $\frac{1}{8}$ in. diam and, after passing through the target and recoil catcher plate, was monitored in the Faraday cup. The recoil nuclei from compound-nucleus reactions are kinematically restricted to relatively small forward angles, and after escaping from the thin target, the recoils traveled in vacuum and were caught on a catcher plate located at a known distance from the target, and oriented in the plane perpendicular to the beam direction. The catcher plate consisted of a 4-in.-diam stainless-steel cutter with sharp circular blades accurately machined at $\frac{1}{8}$-in. radial intervals. Aluminum foil 0.001 in. thick was stretched over the cutting edges, and after collection of recoils the foil was cut into concentric rings by means of an hydraulic press. Each ring corresponded to a well-defined angular interval whose exact value was determined by the calibration procedure described previously.[5] In the present experiments, the target-catcher distance was chosen to yield an angular acceptance of approximately 1.3 deg per ring.

Targets of isotopically separated tin isotopes were used in the angular distribution experiments. Oxides highly enriched in the desired isotope[14] were reduced to metallic tin by fusion with excess potassium cyanide, and the targets were prepared by vacuum evaporation of the tin metal onto preweighed 0.00025-in.-thick aluminum backings. Several batches of targets were made covering the range from about 20 to 100 $\mu g/cm^2$. Individual target thicknesses were determined from the measured weight and area of deposit.

After each bombardment, the catcher foil was cut and the individual rings assayed for 96-min Ba^{126} radioactivity. This was done by counting the high-energy (4.8-MeV) positrons of Cs^{126}, in secular equilibrium with Ba^{126}, through 432-mg/cm² aluminum absorbers in end-window methane gas flow proportional counters. The eight counters used were intercalibrated and adjusted to yield equal counting rates with a thick U^{238} source. The counting of the Ba^{126} samples was followed for several half-lives to ensure purity, or correct for any contaminating activities. As only relative activity measurements were required for each angular distribution, absolute counter-efficiency corrections were not applied to the data.

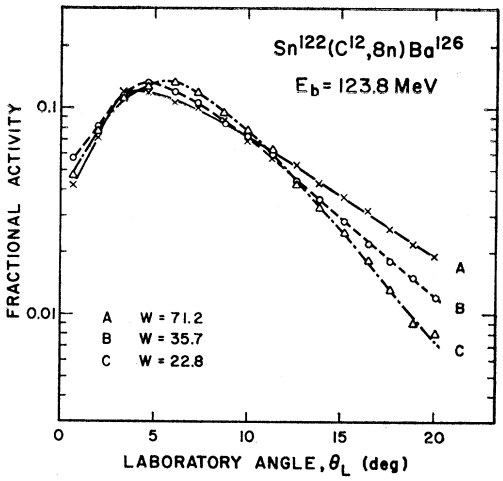

FIG. 1. Typical appearance of Ba^{126} angular distributions from (C^{12}, xn) reactions with Sn isotopes. The three curves are for different target thicknesses as indicated ($\mu g/cm^2$).

The effects of target thickness on the measured angular distributions were determined experimentally by replicate experiments with targets of different thickness. This was done at each bombarding energy with one or more of the target isotopes, permitting extrapolation of the experimental results to zero target thickness. Where the target-thickness dependence was not directly measured for a particular combination of target isotope and beam energy, the appropriate corrections were obtained by interpolation from data of other isotopes or energies. In all cases, the target-thickness corrections were significant but were known with sufficient accuracy to preclude large errors.

RESULTS AND DISCUSSION

Angular distribution experiments were carried out at several bombarding energies from 87.5 to 123.8 MeV. The cylindrical geometry of our apparatus was such that the radioactivity in a catcher ring, at laboratory angle θ_L, is proportional to $d\sigma/d\theta_L$ corresponding to the angular interval subtended by the ring. We have analyzed our data in the following manner. For each ring, we have evaluated σ_i/σ, where σ_i is proportional to the cross section in the angular interval of ring i, and σ is the total cross section. The ratio σ_i/σ is equivalent to the fractional activity found in ring i. The quantity

[13] M. Kaplan and J. L. Richards, Phys. Rev. **145**, 153 (1966).
[14] Obtained from Oak Ridge National Laboratory. The isotopic enrichments were Sn^{118}, 96.26%; Sn^{119}, 83.98%; Sn^{120}, 98.39%; Sn^{122}, 92.25%.

TABLE I. Angular distribution results for Ba^{126} from (C^{12}, xn) reactions with Sn isotopes.

			Angular interval (deg)																	
			0.00	1.35	2.71	4.06	5.40	6.74	8.07	9.39	10.71	12.00	13.30	14.58	15.84	17.10	18.30	19.54	20.70	
			Ring No.																	
Target isotope	Bombarding energy (MeV)	Target thickness ($\mu g/cm^2$)	1	2	3	4	5	6	7	8	9	10	11	12	13	14	15	16	$\langle\theta_L\rangle$ (deg)	$\langle\tan^2\theta_L\rangle$ (10^{-2})
			Fractional cross section σ_i/σ																	
Sn^{122}	123.8	71.2	0.042	0.071	0.119	0.118	0.106	0.100	0.085	0.069	0.058	0.053	0.043	0.037	0.032	0.026	0.022	0.019	8 22	2.94
	123 8	35.7	0.057	0.081	0.117	0.132	0.119	0.104	0.084	0.072	0.059	0.044	0.036	0.028	0.022	0.018	0.015	0.012	7.54	2.50
	123.8	22.8	0.047	0.077	0.114	0.130	0.133	0.118	0.094	0.077	0.060	0.043	0.033	0.025	0.018	0.013	0.009	0.008	7.41	2.33
	111.1	71.2	0.030	0.047	0.070	0.108	0.113	0.105	0.094	0.084	0.073	0.062	0.051	0.043	0.038	0.031	0.027	0.023	9.13	3.42
	111.1	35.7	0.058	0.082	0.111	0.127	0.117	0.099	0.082	0.069	0.058	0.048	0.039	0.032	0.026	0.021	0.016	0.013	7.70	2.62
	111.1	22.8	0.056	0.078	0.104	0.129	0.138	0.120	0.097	0.078	0.054	0.045	0.034	0.023	0.017	0.012	0.009	0.007	7.73	2.28
Sn^{120}	123.8	75.5	0.052	0.065	0.087	0.101	0.103	0.097	0.087	0.077	0.067	0.059	0.050	0.042	0.036	0.030	0.026	0.021	8.70	3.24
	111.1	37.5	0.061	0.080	0.102	0.121	0.125	0.114	0.093	0.076	0.059	0.046	0.037	0.027	0.021	0.016	0.012	0.010	7.53	2.45
	99.6	75.5	0.077	0.100	0.123	0.129	0.119	0.103	0.084	0.068	0.052	0.039	0.032	0.024	0.017	0.014	0.011	0.008	6.96	2.18
	87.5	75.5	0.079	0.111	0.137	0.137	0.127	0.095	0.074	0.058	0.046	0.036	0.028	0.022	0.017	0.014	0.011	0.008	6.69	2.06
Sn^{119}	123.8	67.0	0.049	0.065	0.096	0.103	0.106	0.108	0.096	0.082	0.069	0.055	0.046	0.037	0.029	0.025	0.019	0.016	8.34	2.96
	111.1	67.0	0.058	0.075	0.092	0.103	0.103	0.101	0.093	0.080	0.071	0.058	0.047	0.037	0.028	0.022	0.018	0.014	8.22	2.90
	111.1	47.8	0.052	0.072	0.094	0.111	0.119	0.113	0.096	0.080	0.064	0.052	0.042	0.033	0.026	0.020	0.014	0.013	8.00	2.72
	111.1	25.5	0.058	0.078	0.100	0.116	0.120	0.110	0.093	0.076	0.061	0.049	0.039	0.031	0.024	0.018	0.015	0.011	7.76	2.60
	99.6	67.0	0.083	0.107	0.128	0.135	0.123	0.101	0.077	0.061	0.040	0.031	0.025	0.023	0.020	0.018	0.015	0.013	6.86	2.20
	99.6	47.8	0.077	0.097	0.126	0.137	0.129	0.103	0.083	0.063	0.049	0.037	0.029	0.022	0.017	0.014	0.010	0.008	6.86	2.12
	99.6	25.5	0.083	0.107	0.132	0.138	0.118	0.099	0.077	0.061	0.048	0.037	0.028	0.022	0.018	0.014	0.011	0.008	6.75	2.09
	87.5	67.0	0.081	0.101	0.137	0.154	0.146	0.113	0.081	0.057	0.040	0.028	0.020	0.015	0.011	0.007	0.005	0.004	6.25	1.72
Sn^{118}	123.8	73.0	0.027	0.039	0.061	0.087	0.105	0.105	0.100	0.096	0.087	0.074	0.061	0.048	0.039	0.031	0.022	0.017	9.43	3.53
	111.1	73.0	0.024	0.035	0.048	0.071	0.114	0.130	0.119	0.103	0.081	0.068	0.057	0.049	0.039	0.026	0.021	0.016	9.44	3.47
	99.6	73.0	0.051	0.068	0.088	0.098	0.108	0.092	0.088	0.078	0.074	0.063	0.050	0.043	0.038	0.025	0.020	0.016	8.04	2.77
	87.5	73.0	0.063	0.087	0.111	0.125	0.125	0.111	0.092	0.073	0.057	0.044	0.034	0.026	0.020	0.015	0.011	0.008	7.32	2.33
	87.5	34.5	0.078	0.100	0.123	0.130	0.130	0.107	0.086	0.068	0.052	0.038	0.028	0.020	0.015	0.011	0.008	0.006	6.78	2.05
	87.5	18.8	0.076	0.094	0.117	0.142	0.142	0.110	0.083	0.062	0.047	0.036	0.031	0.021	0.015	0.013	0.008	0.006	6.80	2.05

$\langle\tan^2\theta_L\rangle$ for the angular distribution was then obtained from

$$\langle\tan^2\theta_L\rangle=\sum_i(\sigma_i/\sigma)\langle\tan^2\theta_i\rangle. \quad (1)$$

The factor $\langle\tan^2\theta_i\rangle$ is the average square tangent of the angle subtended by ring i, and is given by[4]

$$\langle\tan^2\theta_i\rangle=\sec\theta_2\sec\theta_1-1, \quad (2)$$

where θ_2 and θ_1 are the defining angles of the ring. We have also computed the average angle $\langle\theta_L\rangle$ for each experiment using the similar relation

$$\langle\theta_L\rangle=\sum_i(\sigma_i/\sigma)\langle\theta_i\rangle;\qquad\langle\theta_i\rangle=\tfrac{1}{2}(\theta_1+\theta_2). \quad (3)$$

The quantity $\langle\tan^2\theta_L\rangle$ is related to the kinematics of the compound-nuclear deexcitation process,[4] and will be used below for interpretation of our results. The average laboratory angle $\langle\theta_L\rangle$ is useful because it gives some physical feeling for the angular distribution.

Our angular distribution data for the four (C^{12}, xn) reactions are presented in Table I. Each experiment corresponds to a horizontal row across the Table. The first three columns list, respectively, the target isotope, bombarding energy, and target thickness in the experiment. Then we show the fractional cross section σ_i/σ measured for each ring. The angular acceptance of each ring is also indicated. Finally, the last two columns contain the average quantities $\langle\theta_L\rangle$ and $\langle\tan^2\theta_L\rangle$ for each angular distribution.

Figure 1 is a typical set of angular distributions for Ba^{126}, obtained at a bombarding energy of 123.8 MeV with Sn^{122} targets of different thickness W. As can be seen the pronounced effect of target thickness is to broaden the angular distribution, presumably by scattering of the recoils into larger angles. Since the computed averages $\langle\tan^2\theta_L\rangle$ are quite sensitive to the cross section at large angles, it is important that these quantities be obtained for zero equivalent target thickness.

The relationships between recoil angular distributions and nuclear reaction dynamics have been presented in detail elsewhere.[3,4] However, for purposes of clarity, we shall outline the arguments here and give the resulting formulas which we shall need. Consider a beam projectile of mass A_b and kinetic energy E_b reacting with a target nucleus of mass A_T to form a compound nucleus. The complete transfer of linear momentum from the incident beam results in a compound-nucleus velocity along the beam direction given by

$$v_c^2=2A_bE_b/(A_b+A_T)^2 \quad (4)$$

(v_c is also the velocity of the center of mass.) The emission of neutrons from the compound system imparts to the residual nucleus a resultant velocity V in the c.m. system, directed at a c.m. angle θ with respect to the incident beam. In the laboratory system, the recoil nucleus will appear at an angle θ_L given by

$$\tan\theta_L=V\sin\theta/(v_c+V\cos\theta). \quad (5)$$

For a large number of recoiling nuclei, the laboratory angular distribution can be characterized by $\langle\tan^2\theta_L\rangle$, which is obtained from Eq. (5) by appropriate averaging and requires specification of $W(\theta)$, the c.m. angular distribution of recoil velocities V. In the present paper, we shall take $W(\theta)$ to be isotropic which leads to the result[4]

$$\langle\tan^2\theta_L\rangle=\sum_{n=1}^{\infty}\frac{2\langle V^{2n}\rangle}{(2n+1)v_c^{2n}}. \quad (6)$$

In Eq. (6), the quantities $\langle V^{2n}\rangle$ are the average $2n$th moments of the resultant velocities (in the c.m. system) imparted to the recoil nuclei by the emission of neutrons. The introduction of these velocity averages is a necessary consequence of there being a distribution in the magnitudes of V.

Equation (6) relates a measurable property of the laboratory angular distribution to the magnitudes of the c.m. velocity v_c and the recoil velocity in the c.m. system V. The former quantity is given by Eq. (4) for compound-nucleus reactions, and is a known quantity in our experiments. On the other hand, the average moments of V are complex quantities, related to the detailed energy and angular distributions of the evaporated particles, and are not generally describable in simple form. Fortunately, however, for compound-nucleus reactions induced by heavy ions, $V\ll v_c$ as a consequence of the large c.m. motion and we need consider only the leading term in Eq. (6). In the case of isotropic neutron emission, it has been shown[3] that

$$\langle V^2\rangle=8T_n/(A_T+A_b+A_R)^2, \quad (7)$$

where T_n is the average total kinetic energy of the emitted particles in the c.m. system and A_R is the mass of the residual nucleus. Combination of Eqs. (4), (6), and (7) yields the relationship

$$T_n=\frac{3E_bA_b(A_b+A_T+A_R)^2}{8(A_b+A_T)^2}\langle\tan^2\theta_L\rangle, \quad (8)$$

which we shall use in the interpretation of our experimental data. Although we are assuming throughout that neutron emission is isotropic, the values of T_n derived from measurements of $\langle\tan^2\theta_L\rangle$ are not very sensitive to the exact form of the angular distribution $W(\theta)$. Even moderate forward-backward peaking does not lead to differences which are experimentally significant,[15] and several studies of heavy-ion-induced reactions have indicated that nucleons are emitted with very little anisotropy.[16–18]

The average total energy dissipated in electromagnetic deexcitation processes may be obtained by subtracting T_n from the total energy available:

$$T_\gamma=(E_{c.m.}+Q)-T_n, \quad (9)$$

[15] A. Ewart and M. Kaplan, Phys. Rev. **162**, 944 (1967).
[16] W. J. Knox, A. R. Quinton, and C. E. Anderson, Phys. Rev. **120**, 2120 (1960).
[17] H. C. Britt and A. R. Quinton, Phys. Rev. **120**, 1768 (1960).
[18] H. W. Broek, Phys. Rev. **124**, 233 (1961).

TABLE II. Average recoil angles and derived average total energies of neutrons and photons for $Sn(C^{12}, xn)Ba^{126}$ reactions.

Reaction	Bombarding energy E_b (MeV)	$\langle\tan^2\theta_L\rangle$ [a] (10^{-2})	Total available energy ($E_{c.m.}+Q$) (MeV)	Average total neutron energy T_n (MeV)	Average total photon energy T_γ (MeV)
$Sn^{122}(C^{12}, 8n)$	123.8	2.00	42.4	42.0	0.4
	111.1	1.76	30.8	33.2	−2.4
$Sn^{120}(C^{12}, 6n)$	123.8	2.24	56.2	47.7	8.5
	111.1	2.06	44.6	39.4	5.2
	99.6	1.94	34.1	33.2	0.9
	87.5	1.62	23.1	24.4	−1.3
$Sn^{119}(C^{12}, 5n)$	123.8	2.07	65.2	44.4	20.8
	111.1	2.27	53.7	43.7	10.0
	99.6	2.00	43.2	34.4	8.8
	87.5	1.33	32.3	20.2	12.1
$Sn^{118}(C^{12}, 4n)$	123.8	2.56	71.8	55.3	16.5
	111.1	2.70	60.3	52.4	7.9
	99.6	2.55	49.8	44.3	5.5
	87.5	1.90	38.8	29.0	9.8

[a] Corrected to zero target thickness.

where $E_{c.m.}$ is bombarding energy in the c.m. system and Q is the over-all reaction mass difference.

Our experimental results for the four neutron-emitting reactions studied are presented in Table II. The values of $\langle\tan^2\theta_L\rangle$ have been corrected to zero target thickness as described earlier, and the average total neutron and photon energies were computed from Eqs. (8) and (9), respectively. The major sources of possible experimental error stem from the target-thickness extrapolations of $\langle\tan^2\theta_L\rangle$ and the uncertainties in beam energy and angular resolution. These combined effects could lead to uncertainties of 2–3 MeV in the derived neutron energies, which are then directly reflected in the photon energies.

In Fig. 2, we have plotted T_n and T_γ as functions of total available energy $E_{c.m.}+Q$ for the $Sn^{122}(C^{12}, 8n)Ba^{126}$, and $Sn^{120}(C^{12}, 6n)Ba^{126}$ reactions. Figure 3 is the corresponding plot for the reaction $Sn^{119}(C^{12}, 5n)Ba^{126}$, and Fig. 4 presents the results for $Sn^{118}(C^{12}, 4n)Ba^{126}$. As these four reactions all lead to the same final product, any significant differences in the division of available energy between neutron and photon emission should be related to the different numbers of neutrons emitted and any local variations in the compound nuclei.

In the reaction $Sn^{122}+C^{12}$ (triangles in Fig. 2) at the two bombarding energies where measurements were made, we observe that all of the available energy is accounted for as kinetic energy of the eight emitted neutrons. These bombarding energies correspond to the steeply increasing portion of the $(C^{12}, 8n)$ excitation function, and it is reasonable to expect that the emitted

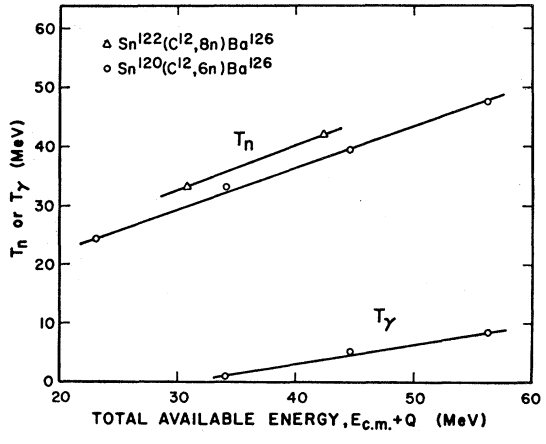

FIG. 2. Average total energies of neutrons T_n and photons T_γ, plotted against total available energy in the c.m. system. The triangles are for the Sn^{122} $(C^{12}, 8n)Ba^{126}$ reaction, and the circles refer to the $Sn^{120}(C^{12}, 6n)Ba^{126}$ reaction.

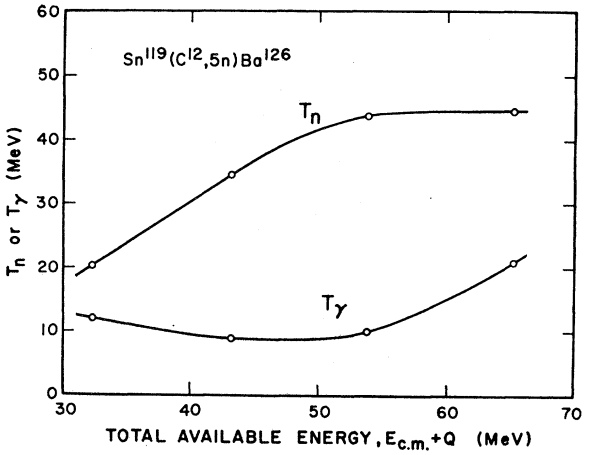

FIG. 3. Average total energies of neutrons T_n and photons T_γ, plotted against total available energy in the c.m. system, for the $Sn^{119}(C^{12}, 5n)Ba^{126}$ reaction.

neutrons will carry essentially all of the available energy. If γ-ray emission were to compete significantly here, it is likely that the resulting energy deficit would prohibit emission of the eighth neutron, and the resulting reaction product would not be observed in our experiments. In other words, we are measuring only a small fraction of the total reaction cross section, namely, those events which require the full energy to occur at all, and it probably involves primarily low-angular-momentum collisions between the beam projectiles and target nuclei.

When the reaction product Ba^{126} is formed by the emission of six neutrons ($Sn^{120}+C^{12}$ reaction), T_n increases approximately linearly with available energy, but γ-ray emission begins to be significant at the higher energies (see circles in Fig. 2). With this (C^{12}, $6n$) reaction at the higher bombarding energies, the cross sections are no longer very small, and γ-ray competition can occur without removing the reaction product from observation. Note that the radiative energy dissipation is increasing with available energy, and at the highest energy obtainable, is comparable to nucleon binding energies. Both the larger cross sections and the increasing γ-ray emission are consistent with the excitation of a greater fraction of high-angular-momentum states in the compound nuclei.

The competition between neutron and photon deexcitation is clearly evident in Figs. 3 and 4, which show the results for the $Sn^{119}(C^{12}, 5n)$ and $Sn^{118}(C^{12}, 4n)$ reactions, respectively. In contrast to Fig. 2, the T_n values increase rapidly at low energies but then tend to level off at the higher available energies. The corresponding values of T_γ are appreciable over the whole energy range covered, and exhibit a strong increase at the higher energies where the neutron energies have slowed their rate of increase. The apparent broad minima in the T_γ functions of Figs. 3 and 4 are just within the range of possible experimental uncertainties, but the systematic trends cause us to believe that they are probably real effects. Such minima could come about from the two types of γ-ray deexcitation predicted by Grover.[10] When the compound nuclei are formed with high excitation energies and angular momenta,[19] γ-ray emission can compete favorably with neutron emission as a consequence of decay through *yrast* levels. At lower excitation energies, the enhanced decay through rotational bands can act as "radiation traps," which would also manifest themselves by increased photon decay at the expense of neutron-evaporation energy. The magnitudes of the total photon energies are large for both reactions, and demonstrates unmistakably the importance of electromagnetic processes in the decay of compound nuclei.

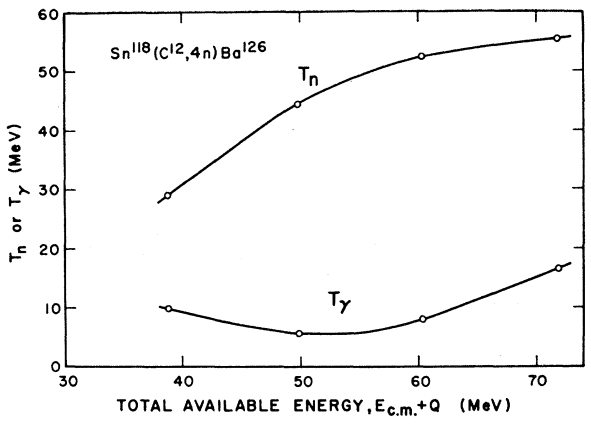

FIG. 4. Average total energies of neutrons T_n and photons T_γ, plotted against total available energy in the c.m. system, for the $Sn^{118}(C^{12}, 4n)Ba^{126}$ reaction.

It is interesting to note that at a given value of the available energy, the magnitude of T_n is lower (and T_γ is higher) for the $Sn^{119}+C^{12}$ reaction compared to the $Sn^{118}+C^{12}$ reaction, even though the former involves the emission of an additional neutron. This is very likely a consequence of the odd and even mass numbers of the respective compound nuclei, as reflected through the differences in angular momenta for *yrast* levels in odd and even nuclei at a given excitation energy.[10]

The results of the present study, combined with other reported measurements of γ-ray competition in specific compound-nucleus reactions,[3–7] serve to indicate that the observed behavior is strongly related to the mass region being investigated, presumably through differences in level densities and availability of angular momentum states at high excitation. Even within a given mass region, one can probably not draw quantitative generalizations without giving detailed consideration to local variations in nuclear structure.

ACKNOWLEDGMENT

We wish to express our appreciation to the operating staff of the Yale HILAC for their efforts in getting beam through our apparatus, and for assistance with the experimental equipment.

[19] In the energy region under consideration, the maximum orbital angular momentum between the beam projectile and target nucleus (calculated in the sharp-cutoff approximation) varies from 50 to 72 $\hbar$ units. This corresponds to average total angular momenta in the compound nuclei of 35–50 $\hbar$ units.